Angiogenesis (2018) 21:335–347
https://doi.org/10.1007/s10456-018-9599-4

ORIGINAL PAPER

Glomerular endothelial cell maturation depends on ADAM10, a key regulator of Notch signaling

Gregory Farber[1] · Romulo Hurtado[1] · Sarah Loh[2] · Sébastien Monette[3] · James Mtui[1] · Raphael Kopan[4] · Susan Quaggin[5] · Catherine Meyer-Schwesinger[6] · Doris Herzlinger[1] · Rizaldy P. Scott[5] · Carl P. Blobel[1,2,7]

Received: 22 June 2017 / Accepted: 8 January 2018 / Published online: 3 February 2018

Abstract

The principal function of glomeruli is to filter blood through a highly specialized filtration barrier consisting of a fenestrated endothelium, the glomerular basement membrane and podocyte foot processes. Previous studies have uncovered a crucial role of endothelial a disintegrin and metalloprotease 10 (ADAM10) and Notch signaling in the development of glomeruli, yet the resulting defects have not been further characterized nor understood in the context of kidney development. Here, we used several different experimental approaches to analyze the kidneys and glomeruli from mice lacking ADAM10 in endothelial cells (*A10ΔEC* mice). Scanning electron microscopy of glomerular casts demonstrated enlarged vascular diameter and increased intussusceptive events in *A10ΔEC* glomeruli compared to controls. Consistent with these findings, genes known to regulate vessel caliber (Apln, AplnR and Vegfr3) are significantly upregulated in *A10ΔEC* glomeruli. Moreover, transmission electron microscopy revealed the persistence of diaphragms in the fenestrae of *A10ΔEC* glomerular endothelial cells, which was corroborated by the elevated expression of the protein PLVAP/PV-1, an integral component of fenestral diaphragms. Analysis of gross renal vasculature by light sheet microscopy showed no major alteration of the branching pattern, indicating a localized importance of ADAM10 in the glomerular endothelium. Since intussusceptions and fenestrae with diaphragms are normally found in developing, but not mature glomeruli, our results provide the first evidence for a crucial role of endothelial ADAM10, a key regulator of Notch signaling, in promoting the development and maturation of the glomerular vasculature.

Keywords Glomeruli · Endothelial cells · A disintegrin and metalloprotease 10 (ADAM10) · Notch · Fenestra · Diaphragms

Introduction

The specialization of organ-specific vascular beds is crucial to support the proper perfusion and function of all major organs. Individual vascular beds often develop specific morphological and structural features that aid in their

Electronic supplementary material The online version of this article (https://doi.org/10.1007/s10456-018-9599-4) contains supplementary material, which is available to authorized users.

✉ Carl P. Blobel
blobelc@hss.edu

[1] Department of Physiology, Biophysics and Systems Biology, Weill Cornell Medicine, New York, NY, USA

[2] Arthritis and Tissue Degeneration Program, Hospital for Special Surgery, S-Building, Room 702, 535 East 70th Street, New York, NY, USA

[3] Laboratory of Comparative Pathology, Memorial Sloan Kettering Cancer Center, The Rockefeller University, Weill Cornell Medicine, New York, NY, USA

[4] Division of Developmental Biology, Cincinnati Children's Hospital Medical Center, University of Cincinnati College of Medicine, Cincinnati, OH, USA

[5] Feinberg Cardiovascular Research Institute and Division of Nephrology and Hypertension, Northwestern University, Chicago, IL, USA

[6] Department of Nephrology, University Medical Center Hamburg-Eppendorf, Hamburg, Germany

[7] Institute for Advanced Study, Technical University Munich, Munich, Germany

specialized function. The renal vasculature is a sophisticated and complex network of blood vessels that transports blood to individual glomeruli, highly convoluted and fenestrated capillary tufts where fluids, salts and soluble materials in the blood undergo the first filtration step in the production of urine. The glomerular microvasculature is fed by an afferent arteriole and drains into an efferent arteriole. About 20% of the total blood flow passes through glomeruli at any given time, which function as sites of filtration due to their highly specialized filtration barrier. This barrier is composed of a fenestrated endothelium, a glomerular basement membrane and interdigitating foot processes of morphologically unique perivascular cells named podocytes. During development, each glomerulus is thought to arise from small clusters of endothelial cells that divide to generate the mature vascular structure through coordinated interactions with podocytes and mesangial cells [1]. Our current understanding of the signaling pathways that drive the establishment of the glomerular endothelium is far from complete, and we know very little from previous studies what signaling events regulate and drive its maturation.

The formation of the glomerular vasculature begins with the recruitment of glomerular endothelial cells into the vascular cleft of a developing glomerulus. This process depends on vascular endothelial growth factor (VEGF) signaling [2]. The recruited endothelial cells initially form a single capillary loop, which then gives rise to additional loops through intussusception, ultimately producing a mature glomerular capillary tuft [3]. During maturation of the glomerular vasculature, the glomerular endothelial cells transition from diaphragmed to non-diaphragmed fenestrated capillaries [4]. The VEGF pathway is involved in the acquisition of the endothelial fenestrae and presence of fenestral diaphragms [5, 6]. Moreover, Norrin, Frizzled4 and the Wnt pathway [7] as well as the Notch signaling pathway [8–10] have been implicated in the regulation of plasmalemma vesicle-associated protein (PLVAP), an integral protein in fenestral diaphragms, during development of the blood–brain barrier [7]. The development of capillary loops that form a glomerular vascular tuft requires platelet-derived growth factor B (Pdgfb) [11], and Notch signaling is crucial for podocyte and mesangial cell maturation [12, 13].

Previous studies have shown that conditional inactivation of ADAM10 in mouse endothelial cells results in enlarged kidney glomeruli compared to controls [14]. ADAM10 is a cell surface metalloprotease that is required for activation of Notch by processing the membrane-proximal extracellular cleavage site, referred to as the S2 site, of this membrane-anchored transcription factor [15, 16]. Therefore, inactivation of ADAM10 typically results in a block of Notch signaling [14, 17–19]. With respect to the glomerular vasculature, this was corroborated by the observation that similar glomerular defects to those seen upon inactivation of ADAM10 in endothelial cells were observed in mice lacking Notch1 in endothelial cells and Notch4 systemically [19]. Moreover, overexpression of the Notch intracellular domain rescued the defects observed in mice lacking ADAM10 in endothelial cells [19]. Taken together, these findings indicate that ADAM10-dependent Notch signaling in glomerular endothelial cells plays an important role in glomerular development or homeostasis or both.

Since ADAM10/Notch signaling regulates the endothelial tip- versus stalk cell fate decision during retinal angiogenesis [20–23], and Notch signaling regulates cell fate decisions in other vascular beds, such as in long bones [24, 25] and in the liver [26], we hypothesized that ADAM10/Notch signaling controls the cell fate of glomerular endothelial cells to regulate their maturation and specialization. To learn more about the consequences of inactivating ADAM10 in endothelial cells for the glomerular vasculature, we analyzed mutant and control glomeruli using transmission and scanning electron microscopy and performed immunofluorescence and histochemical analysis for specific markers of the different cell types in glomeruli. Moreover, we analyzed the kidney and glomerular vasculature using a combination of lectin perfusion and light sheet microscopy and used urine and serum analysis to evaluate kidney function. Finally, we explored how inactivation of ADAM10 in endothelial cells affects the expression of markers of glomerular specialization. Our results provide the first evidence for a critical role of endothelial ADAM10/Notch signaling in controlling the proper development and maturation of the glomerular vasculature.

Results

Scanning electron microscopic analysis of glomerular vascular corrosion casts reveals an increase in intussusceptive events and in vascular diameter

In order to examine the morphology of the glomerular vasculature in 6-week-old *Adam10flox/flox-Tie2-Cre* mice (referred to as *A10ΔEC* throughout), we generated vascular corrosion casts of the kidney vasculature from mutant mice and wild-type controls and subjected these to scanning electron microscopy (Fig. 1, wild-type control, a and b; *A10ΔEC*, c and d, see materials and methods for details). An analysis of the glomerular corrosion casts showed that the mutant animals had nearly double the number vessels with a diameter of six microns or larger, whereas the average vessel diameter of control animals was approximately 5 microns (Fig. 1e). The glomerular vessels found in the mutant animals were on average about 8%

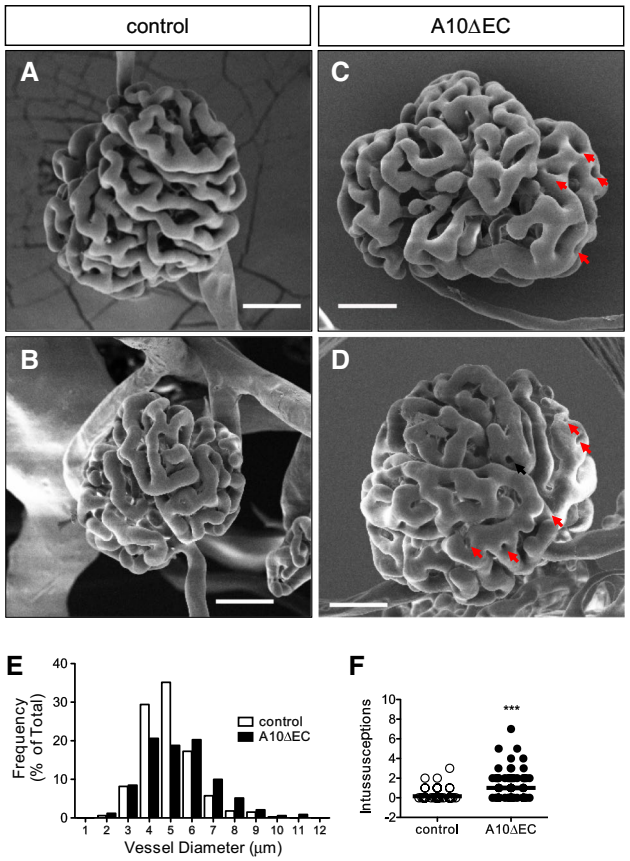

Fig. 1 Scanning electron microscopic analysis of glomerular vascular corrosion casts reveals an increase in intussusceptive events and in vascular diameter. **a**, **b**, **c**, **d** Scanning EM images of a control (**a**, **b**) and *A10ΔEC* glomerulus (**c**, **d** red arrows indicate holes that were scored as likely intussusceptive events). **e** Histogram of capillary vessel diameters. **f** Relative number of glomeruli with zero to seven intussusceptive capillary loops visible on one hemisphere for control ($n = 108$) and *A10ΔEC* animals ($n = 109$). p value < .0001

larger in diameter than in littermate controls (Supplemental Figure 1). These data provide quantitative evidence that the loss of ADAM10 in endothelial cells results in glomeruli with dilated vessels [14]. Interestingly, we found that the glomeruli of the mutant mice ($n = 109$) had on average one well-defined intussusceptive event per hemisphere, whereas these intussusceptions were lacking in controls ($n = 108$, Fig. 1a–d, the two examples shown have several intussusceptions, marked by red arrows; quantification in Fig. 1f). Since intussusceptive events are known to contribute to the development of vascular loops during the development of the glomeruli, these findings suggest that ADAM10/Notch signaling regulates intussusceptive events and vascular diameter.

Transmission electron microscopic analysis of *A10ΔEC* glomeruli shows persistence of diaphragms in the fenestra of glomerular endothelial cells

The presence of fenestrae is a characteristic feature of glomerular endothelial cells whose appearance changes during glomerular development [4], prompting us to evaluate whether ablation of ADAM10 affected this specialized vascular structure by transmission electron microscopy (TEM, Fig. 2). Low-magnification images provided additional evidence for enlarged glomerular vessels in *A10ΔEC* mice compared to controls (Fig. 2a, b, enlarged vessels marked by red asterisks in b). Higher-magnification images revealed that the glomerular endothelial fenestrae of *A10ΔEC* mice contained electron dense material, suggesting the presence of fenestral diaphragms (Fig. 2d, f, red arrows), that was not present in littermate control fenestrae (Fig. 2c, e, yellow arrows; see Supplemental Figure 3 for higher-magnification SEM images) [4]. Quantification of fenestrae with electron dense material resembling diaphragms showed that control glomeruli only exhibited an average of 6.4% fenestrae with putative diaphragms (standard deviation of 5.8%), whereas *A10ΔEC* glomeruli exhibited 65.7% fenestrae with structures resembling diaphragms (standard deviation of 8%; Fig. 2g). By contrast, there were no evident differences in the diameter of fenestral pores (Fig. 2h, supplemental Figure 2) or in the thickness or appearance of the glomerular basement membrane between *A10ΔEC* and controls (Fig. 2, labeled GBM in e, f). Moreover, the podocyte foot processes also had a comparable appearance with respect to their spacing, width and overall arrangement along the basement membrane in *A10ΔEC* and wild-type controls (Fig. 2, labeled Pod in c, d, e, f). These findings provide the first evidence to suggest a role of ADAM10 in promoting the transition from fenestra with diaphragms to open fenestra without diaphragms during maturation of glomerular endothelial cells.

Immunofluorescence analysis of glomeruli with markers for endothelial cells, podocytes and mesangial cells illustrates no major changes in the composition of these major glomerular cell types

To further explore whether the lack of ADAM10 affected the appearance or distribution of endothelial cells, podocytes and mesangial cells in *A10ΔEC* glomeruli compared to controls, we performed immunofluorescence analysis with markers for endothelial cells (endomucin) and mesangial cells (PdgfrB, Fig. 3a) or podocytes (nephrin, marker of the slit-diaphragm bridging podocyte foot processes, Fig. 3b). The overall distribution of mesangial cells (Fig. 3a) or podocytes (Fig. 3b) among the endomucin-labeled endothelial

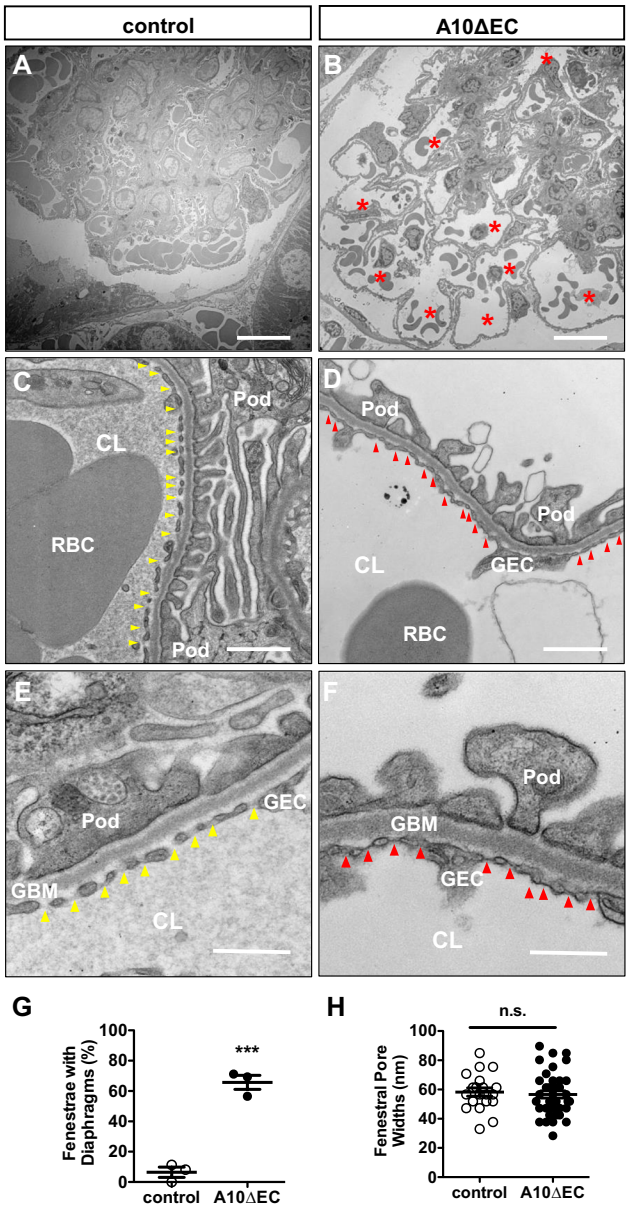

Fig. 2 Transmission electron microscopic analysis of A10ΔEC glomeruli shows persistence of electron dense material resembling diaphragms in the fenestra of glomerular endothelial cells. **a**, **b** Low-magnification images of normal and *A10ΔEC* glomeruli. Red asterisks in **b** indicate dilated glomerular capillary loops. **c**, **e** TEM of control glomerular endothelial fenestrae. Normal open fenestrae indicated by yellow arrows in **e**. **d**, **f** TEM images of *A10ΔEC* glomerular endothelial fenestrae show the presence of electron dense material that is consistent with the presence of fenestral diaphragms in panels **f** (red arrows point to the apparent diaphragms spanning fenestrae in *A10ΔEC* glomerular endothelial cells). Scale bars **a**, **b**: 10 microns. **c**, **d**: 1 micron. **e**, **f**: 500 nm. *Pod* podocytes, *GBM* glomerular basement membrane, *GEC* glomerular endothelial cell, *CL* capillary lumen, *RBC* red blood cell. **g** Quantification of percent fenestrae with apparent diaphragms (*p* value .0005). **h** Quantification of the shortest diameter of fenestrae from tangential pore images (see Supplemental Figure 2 for example)

cells was comparable between *A10ΔEC* and control glomeruli (see merged images in Fig. 3a, b). In Fig. 3a, white arrows in the merged images point toward PdgfrB-positive mesangial cells that are interspersed between endomucin-positive glomerular endothelial cells. In Fig. 3b, white arrows point toward nephrin-positive podocytes that are surrounded by endomucin-positive glomerular endothelial cells. Thus, there were no evident abnormalities in the distribution of mesangial cells and podocytes in the glomeruli of *A10ΔEC* mutants compared to control glomeruli.

Comparable recruitment of endothelial cells into the vascular cleft at different stages of glomerular development

Kidneys of newborn (P0) mice contain all stages of glomerular development, providing an opportunity to examine the morphology of developing glomeruli. VEGF-A is known to recruit endothelial cells into the developing glomerulus during the S-shaped body stage of glomerular development. Since VEGF-A is an upstream regulator of Notch signaling [27], we evaluated whether the recruitment endothelial cells into the cleft is affected in *A10ΔEC* mice. However, we found a similar appearance and pattern of CD31 (PECAM)-positive endothelial cells in sections of three different representative stages of glomerular development [11], S-shaped bodies, maturing glomeruli or mature glomeruli, in newborn *A10ΔEC* samples compared to controls (Fig. 4).

Light sheet microscopy of the kidney vasculature of newborn (P0) mice reveals a normal arterial branching pattern in A10ΔEC animals

Since ADAM10/Notch signaling controls the branching pattern and vascular density during developmental retinal angiogenesis [14, 19–23], we were interested in determining whether ablation of endothelial ADAM10 affects the branching pattern or vascular density of the kidney arterial vascular tree. We therefore performed light sheet microscopy on newborn (P0) kidneys that were perfused with fluorescently tagged tomato lectin. Since arteriole branching is largely completed at P0, analysis at this time point provides insights into the overall branching pattern of the kidney vasculature. To assess branching, we digitally removed all smaller vessels, such as those to the left of the dotted line in the image of a wild-type kidney shown in Fig. 5a (Supplemental Figure 4 has a link to a representative video of a perfused kidney). This allowed for the visualization of the main branches of the kidney vascular tree (Fig. 5b). We found no evident major changes in the overall three-dimensional vascular architecture of the perfused larger vessels, and no difference in the number of main vessel branches between mutant and wild-type animals (Fig. 5b for representative images and

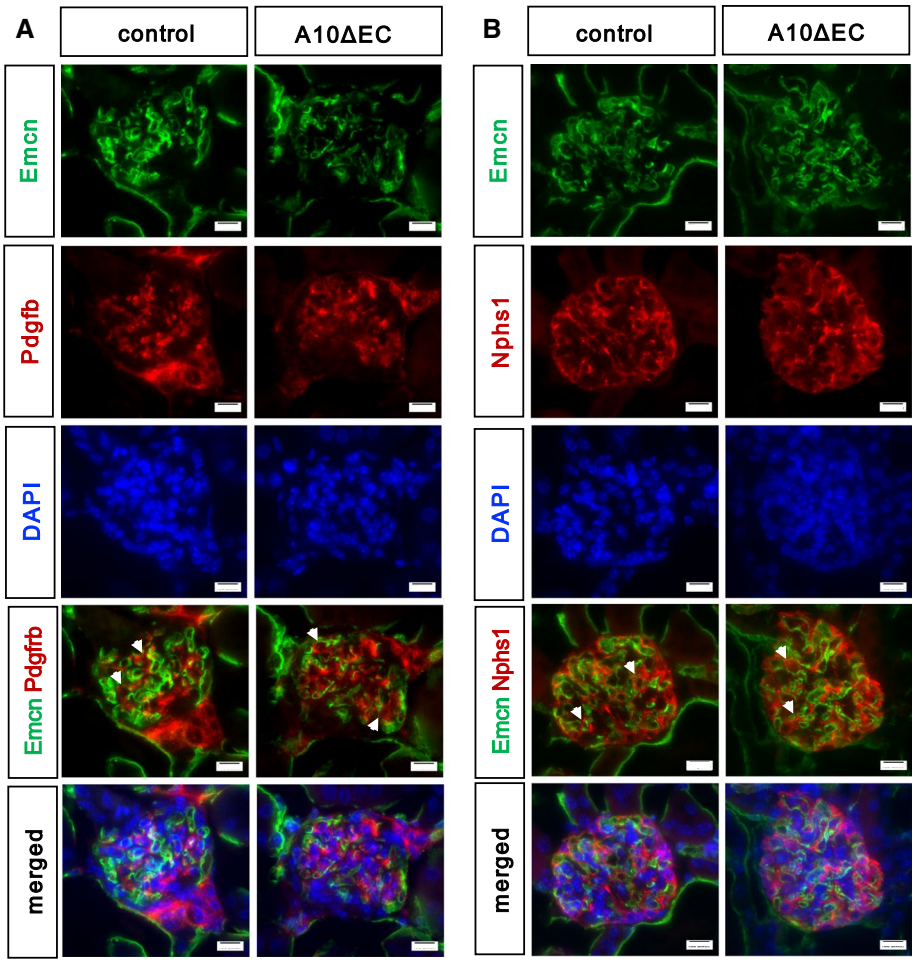

Fig. 3 Immunofluorescence analysis of glomeruli with markers for endothelial cells, podocytes and mesangial cells did not uncover major evident changes in the composition of glomerular cells. Staining for nuclei (DAPI), endothelial cells (Endomucin, Emcn), **a** mesangial cells (PdgfrB), **b** podocyte staining (Nephrin, Nphs1) and combined staining with these markers on control (left panels) and *A10ΔEC* glomeruli (right panels). Images were acquired using a 60× objective. White arrows in combined images point to representative areas were cell interactions appear normal when compared to control glomeruli. Scale bars: 11 µm

5C for quantification). These results indicate that the main vascular defects in the kidney in A10ΔEC mice are restricted to the glomeruli.

qPCR analysis of glomeruli shows altered expression of genes involved in regulating vessel diameter and fenestral diaphragm formation

In order to evaluate potential changes in gene expression in mutant versus control glomeruli, we used a modified fine mesh sieve to isolate intact glomeruli and enrich for glomerular endothelial cells [28] (see materials and methods for details). This approach separates glomeruli from the surrounding kidney tissue, thereby helping to reduce signals arising from the main kidney vessels (i.e., arterioles and venules). Our analysis focused on the expression of genes related to the production and persistence of diaphragms or in regulating vascular diameter in glomerular cDNA by qPCR. We found a significant upregulation of the plasmalemma vesicle-associated protein (PLVAP, also referred to as PV-1) in *A10ΔEC* mice (Fig. 6a). PLVAP is a key component of fenestral diaphragms [29, 30], which supports the conclusion that the increase of electron dense material found in the TEM analysis represents diaphragmed fenestrae. The increased expression of PLVAP in *A10ΔEC* mice was further corroborated by immunohistochemistry, which showed strong immunostaining with anti-PLVAP in *A10ΔEC* glomeruli, but not in controls (Fig. 6c). In addition, we observed an increase in the mRNA expression of apelin and the apelin receptor (regulators of vessel caliber [31–33]), and the Vegfr3, which is regulated by Notch in endothelial cells [34]. Finally, we found a significantly decreased expression of Cxcr4, implicated in regulating glomerular capillary size [35], with no significant change in the expression of its ligand, Cxcl12 (Fig. 6b).

Analysis of urine or serum in adult A10ΔEC mice showed no major deficiencies in kidney function

To determine whether the presence of glomerular fenestral diaphragms or the abnormal glomerular vascular morphology affects kidney function, we analyzed serum and urine from 8-week-old mutant and wild-type mice.

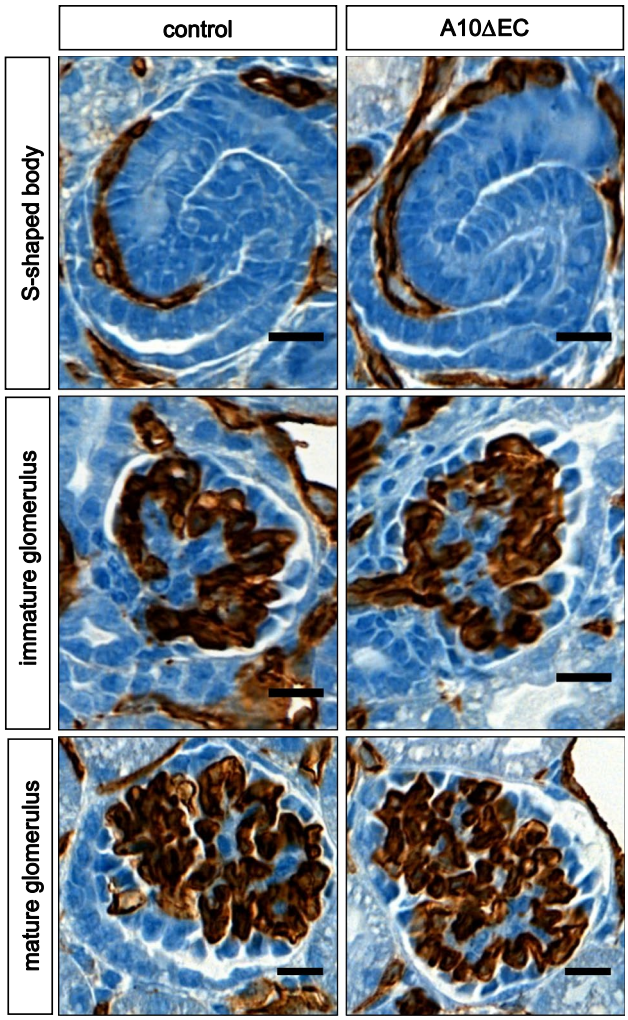

Fig. 4 Comparable recruitment of endothelial cells into the vascular cleft at different stages of glomerular development. PECAM (CD31) staining of kidneys isolated from newborn controls or *A10ΔEC* mice show comparable staining patterns at different stages of maturation, the S-shaped body (top row), the maturing glomerulus (middle row) and a mature glomerulus (bottom row). Representative samples for sections from 3 different litters with mutant and control littermates are shown. Scale bars: 12.5 µm

The *A10ΔEC* mice, which show no increase in mortality until after 10 weeks of age [14], showed no statistically significant changes in electrolytes in serum, in serum creatinine and serum BUN compared to controls (Table 1). No qualitative difference was seen in urine samples separated by SDS-PAGE (Supplemental Figure 5). The urine albumin-to-urine creatinine ratio was normal in *A10ΔEC* mice when compared to controls (Table 1), so there was no evidence for significant albuminuria. The lower levels of serum albumin observed in *A10ΔEC* mice (Table 1) were therefore most likely not caused by abnormal kidney function.

Discussion

The main goal of this study was to provide a better understanding of the role of ADAM10/Notch signaling in endothelial cells in the development of the glomerular vasculature. Previous studies had shown that inactivation of ADAM10 or Notch signaling in endothelial cells results in enlarged glomeruli [14, 19], yet little was known about the vascular defects with regard to kidney development and whether they have functional consequences. Here, we establish for the first time that endothelial ADAM10, an essential regulator of Notch signaling [14, 19], plays a critical role in promoting the maturation of glomerular endothelial cells from an immature stage, in which glomeruli contain intussusceptions and enlarged vessels that have fenestra with diaphragms, to their mature morphology with normal vessel size, lack of intussusceptions and open fenestra without diaphragms.

The maturation of glomeruli begins after the first capillary loops form (capillary loop stage) [1, 11]. During further maturation, additional capillaries branch out from the original single capillary. This is thought to depend, at least in part, on vascular intussusception, the formation of pillar-like connections between opposing endothelial cell walls. Intussusception can initiate a new vascular branch and is considered a normal intermediate in glomerular development [36]. Interestingly, there was a significant increase in glomeruli with apparent intussusceptive events as well as in the number of intussusceptive events per glomerulus in *A10ΔEC* animals. This is consistent with a defect in glomerular maturation in *A10ΔEC* animals, although increased intussusception can also occur as part of a repair mechanism for damaged glomeruli, such as in mesangioproliferative glomerulonephritis [37].

Scanning electron microscopy showed enlarged diameters of capillaries in *A10ΔEC* glomeruli. Interestingly, we found increased expression of apelin and its receptor AplnR, which regulate endothelial cell proliferation and vessel diameter expansion during development [31–33]. Moreover, we found increased expression of the Vegfr3, which is expressed on fenestrated endothelial cells [38]. The Vegfr3 and Vegfr2 have been linked to Notch signaling in retinal endothelial cells [39], and the Vegfr3 regulates vessel caliber and acts as a sensor for fluid shear stress [40]. Therefore, Vegfr3 upregulation is consistent with vascular remodeling caused by altered flow and shear stress in the mutant glomerular capillaries, which could also be involved in triggering intussusception [41]. Finally, *A10ΔEC* glomeruli have decreased expression of Cxcr4, the receptor for Cxcl12/Sdf-1. Interestingly, Cxcr4 endothelial-specific knockout mice also have enlarged glomerular capillaries [35]. Taken together, these findings

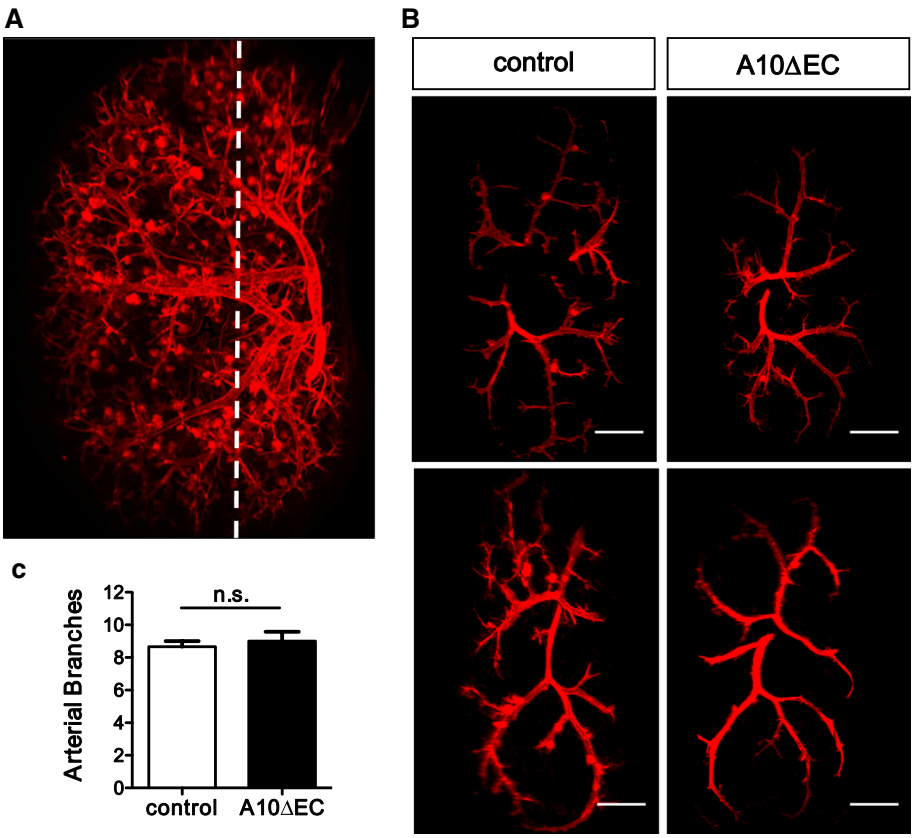

Fig. 5 Light sheet microscopy of the kidney vasculature of newborn (P0) mice reveals a normal arterial branching pattern in A10ΔEC animals. **a** A representative image of a kidney from a newborn (P0) *A10ΔEC* mouse perfused with fluorescently tagged tomato lectin. Kidneys were cleared using the iDisco clearing protocol and imaged using a light sheet microscope (see materials and methods for details). Scale bars: 200 µm. **b** Pruned kidney vascular trees, in which the smaller vessels on the left of the dotted white line shown in A were digitally removed to highlight the branching pattern of the major arteries, scale bars: 227 µm. **c** The main vascular branches were counted to assess possible changes in overall branching pattern of the large arteries and arterioles

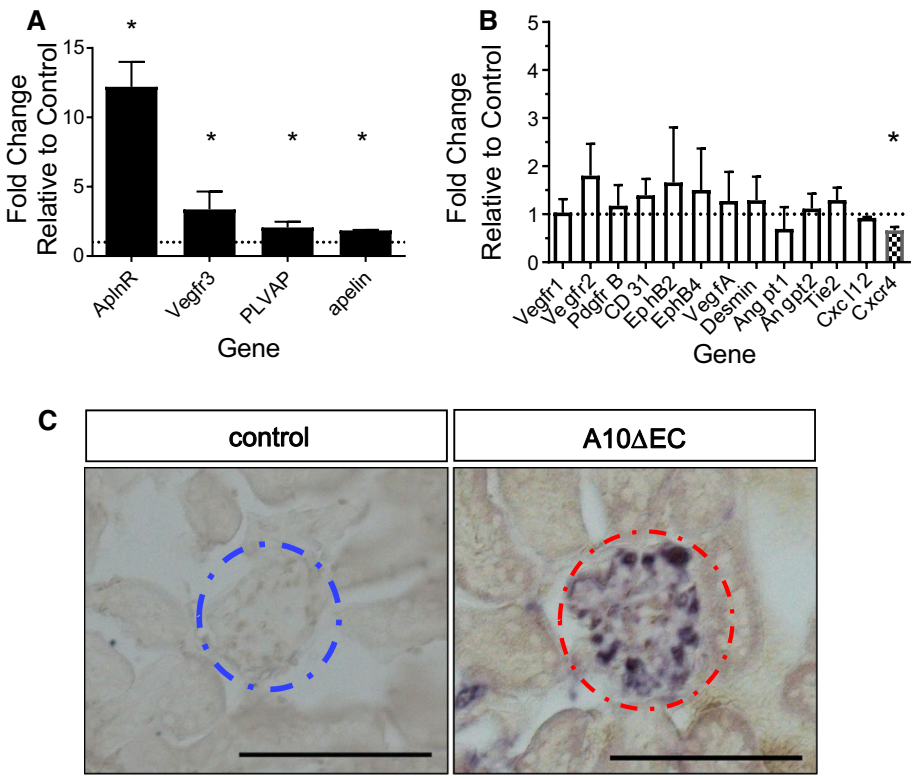

Fig. 6 qPCR analysis of glomeruli shows altered expression of genes involved in regulating vessel diameter and fenestral diaphragm formation. A) qPCR analysis of cDNA samples generated from glomeruli that had been enriched using the sieve method of glomerular isolation. Apelin and the apelin receptor (AplnR), Vegfr3 and plasmalemma vesicle-associated protein (PLVAP, PV-1) were expressed at significantly higher levels in the mutant samples compared to controls. (*p* values, respectively, .0004; .0327; .0108; and < .0001) **b** Cxcr4 was expressed at a statistically lower level (*p* value .0011). *Indicates a *p* value < 0.05. **c** Representative images of glomeruli stained with anti-PLVAP antibody. The presence of anti-PLVAP is indicated by dark purple staining, and glomeruli are circled in blue (control) and red (*A10ΔEC*). Scale bar represents 100 microns

Table 1 Urine and serum analysis in adult A10ΔEC mice showed no major deficiencies in kidney function

	Control		A10ΔEC	
	Mean value	SEM	Mean value	SEM
Serum creatinine (mg/dL)	0.30	0.03	0.29	0.03
Serum BUN (mg/dL)	28.85	1.41	31.60	1.75
Urine albumin/creatinine (g/g)	0.23	0.03	0.25	0.04
Serum albumin (g/L)	17.46	0.60	14.64*	0.41
Serum sodium (mM)	155.60	0.72	155.70	0.69
Serum potassium (mM)	8.22	0.24	8.84	0.23
Serum chloride (mM)	113.80	1.01	114.60	1.15
Serum calcium (mM)	2.80	0.03	2.85	0.05

Analysis of serum creatinine and serum BUN showed no statistically significant difference between mutant and control animals. Also, there was no significant difference in the urinary albumin-to-creatinine ratio in control vs *A10ΔEC* mice. However, serum albumin showed a significant reduction in *A10ΔEC* mice compared to controls, possibly because of impaired production of albumin in the liver, which also has significant vascular abnormalities [14, 19]. There appeared to be no statistically significant change in urine sodium, potassium, chloride and calcium ion concentration

provide the first evidence that ADAM10/Notch signaling regulates the expression of several molecules in glomeruli, whose dysregulation could explain the increased vascular diameter and intussusceptive events in *A10ΔEC* glomeruli.

When we performed light sheet microscopy to visualize the 3-dimensional glomerular vascular tree, we found no evident vascular defects in *A10ΔEC* kidneys. This suggests that inactivation of ADAM10 with the Tie2-Cre, which occurs around embryonic day E12.5 [19], results in defects that are restricted to specialized vascular structures, such as glomeruli, liver sinusoids or coronary vessels, without causing evident morphological defects in other parts of the vasculature [14, 19]. This conclusion is further supported by a histological analysis of kidneys of from 12- and 3.5-week-old mice, in which all parts except for the glomeruli appeared normal in *A10ΔEC* mice (Supplemental Figures 6 and 7).

During glomerular development, glomerular endothelial cells undergo several stages of maturation [4]. Initially, they develop vesicular structures under their plasma membrane that are lined with fenestral diaphragms [4], indicative of an intermediate stage of maturation. Fenestral diaphragms are lost during the maturing glomerulus stage, so that mature glomerular endothelial cells carry open fenestrae without diaphragms. The presence of electron dense material resembling fenestral diaphragms in our TEM analysis together with the upregulation of the fenestral diaphragm marker PLVAP [30] suggests that the glomerular maturation in *A10ΔEC* animals is arrested or at least delayed at an immature state. Despite the apparent persistence of fenestral diaphragms, there were no major functional consequences, at least as indicated by a normal urine creatinine and albumin ratio and normal urine and serum electrolytes. Since little is known about how diaphragms affect kidney function, these findings indicate that the apparently persisting diaphragms do not interfere with the selective permeability of the glomerular filtration barrier. One possibility is that the loss of PLVAP and diaphragms during glomerular maturation represents a fluid flow adaptation to maintain flow from the capillary endothelium to the urinary Bowman's space despite mounting resistance caused by increased complexity of the GBM and the formation of podocyte slit diaphragms during development. Interestingly, PLVAP is among genes upregulated in endothelial cells subjected to sustained fluid shear stress [42], and it has previously been shown to be regulated by Notch signaling [8–10].

Lack of Notch signaling in early embryonic development affects the decision between arterial and venous endothelial cell fate, leading to reduced expression of the arterial marker EphB2 [43]. However, we did not see a significant difference in EphB2 or EphB4 expression in *A10ΔEC* glomeruli samples compared to controls, suggesting that arterial/venous specification in glomeruli is not significantly affected in *A10ΔEC* mice. Instead, ADAM10/Notch is most likely required for the later differentiation steps described here.

In summary, we used *A10ΔEC* mice to analyze the glomerular defects previously observed *A10ΔEC* mice or *NotchΔEC* in more detail [14, 19]. This uncovered a novel role for endothelial ADAM10, a key regulator of Notch signaling, in promoting the normal development of glomerular endothelial cells. We propose that the higher expression of apelin and its receptor, of the Vegfr3, of PLVAP and the apparent presence of diaphragms, and the decreased expression of Cxcr4 in glomerular endothelial cells in *A10ΔEC* mice define an immature state of glomerular development. We hypothesize that the role of ADAM10-dependent Notch signaling in the maturation of glomerular endothelial cells is conceptually similar to the role of ADAM10/Notch signaling in cell fate decisions. In glomeruli, normal ADAM10/Notch signaling would then promote the full maturation of glomeruli by downregulation of apelin and its receptor, of Vegfr-3, and PLVAP, which was previously shown to be regulated by Notch signaling [8–10], and upregulation of Cxcr4, resulting in the disappearance of diaphragms and a normal vessel diameter. In addition, the increased intussusceptive events in *A10ΔEC* glomeruli are also consistent with a less mature state [36]. Taken together, these studies provide new insights into the role of glomerular endothelial ADAM10/Notch signaling in regulating the proper development of glomeruli.

Methods

Materials

The following antibodies were used in this study. Anti-endomucin (Ab106100) was used at 1:400; anti-nephrin (AF3159) was used at 5ug/ml; anti-PdgfrB (ab32570) was used at 1:100; anti-PLVAP (BD Biosciences 550563) was used at 1:10; and donkey anti-rat 594 (A-21209) and donkey anti-goat (A-21447) were both used at 1:250. The anti-CD31 antibody was from Dianova (# DIA-310). The secondary antibody for PLVAP was goat anti-rat 2-AP (Santa Cruz #sc-3824) and was used at 1:1000.

Mice

The mouse strains used here have been previously described [14]. Briefly, mixed background female mice (129 Sv/C57Bl6) carrying two floxed alleles of ADAM10 were mated with male mice carrying two floxed alleles of ADAM10 and the Tie2-Cre transgene for inactivation of ADAM10 in endothelial cells. All comparisons were between mice carrying the two floxed alleles and the Tie2-Cre transgene (A10ΔEC mice) and their littermate controls without the Tie2-Cre transgene (ADAM10flox/flox mice), which had previously been shown to resemble wild-type mice in that they have no evident spontaneous pathological phenotypes [14]. In most experiments, the mutant and control mice were 6 weeks old, except for the animals used in Supplemental Figures 6 and 7, which were either 3.5 or 12 weeks old, and except for the newborn mice used in Figs. 4 and 5 and Supplemental Figure 4. All procedures were approved by the Animal Care and Use Committee of the Hospital for Special Surgery and of Weill Cornell Medicine.

Corrosion casting and scanning electron microscopy of adult kidney tissue

Three littermate gender matched pairs of 6-week-old mice with each pair consisting of one mutant and one control animal (total of 6 animals; 4 males and 2 females) were euthanized using carbon dioxide euthanasia and then perfused with 20 ml of PBS with 200 USP units of heparin using a solution that was pre-warmed to 37 °C. The perfusion mixture was injected through the left ventricle and an incision made in the right atria to release the injected fluid. A successful perfusion was indicated by a slow clearance of red blood cells from the kidney, as indicated by a change in the color of the kidney tissue. After flushing out the blood, the mouse was injected with 10 ml of corrosion casting solution (Batson's No. 17 Corrosion Kit) at 1 ml/minute through the left ventricle of the heart. The casting solution was left to cure for at least 2 h at room temperature; then, the organ was digested with 20% KOH and washed with water until the tissue was fully dissolved, leaving only the corrosion cast. Select regions of a cast were then mounted and sputter-coated with 2 nm of iridium using a Leica ACE600. Samples were then imaged using a Zeiss LEO 1550 scanning electron microscope.

Quantification of corrosion cast structures and vessel diameter

Selected images were analyzed using Adobe Photoshop. Glomeruli were analyzed in a blinded manner for the presence or absence of small round holes that resembled intussusceptive events per glomerulus and for the number of such intussusceptive events per glomerulus. Moreover, the diameter of at least 3 of the apparently largest blood vessels per glomerulus was recorded. For this, only vessels were chosen for which the complete diameter was visible in the image. The diameter was defined as the perpendicular distance from one side of the vessel to the other.

Transmission electron microscopy of kidney tissue

Tissues from six mice (3 mutant and 3 control, 4 males and 2 females, littermate and gender matched) that were 6 weeks of age were washed with PBS and then fixed with a fixative of 2.5% glutaraldehyde, 4% paraformaldehyde and 0.02% picric acid in 0.1 M sodium cacodylate buffer at pH 7.2. Samples were then fixed in 1% osmium tetroxide and 1.5% potassium ferricyanide. Next, the samples were dehydrated through a graded ethanol series and embedded in an Epon analog resin. Ultrathin sections of 60–80 nm thickness were cut using a Diatome diamond knife (Diatome, USA, Hatfield, PA) on a Leica Ultracut S Ultramicrotome (Leica, Vienna, Austria). Sections were collected on copper grids and further contrasted with lead citrate and viewed on a JEM 1400 electron microscope (JEOL, USA, Inc., Peabody, MA) operated at 100 kV. Images were recorded with a Veleta 2 K × 2 K digital camera (Olympus-SIS, Germany). Images were taken at 15,000×, 30,000× and 60,000× zoom. Sample preparation was performed by the Weill Cornell Medicine Imaging Core Facility staff.

Quantification of fenestral diaphragms

To quantify the number of fenestrae with diaphragms, high-magnification transmission electron microscopy images were selected for each litter pair, with a total of 3 pairs of mutant and control mice analyzed, and each pair from a different litter. A minimum of 5 images showing fenestrated endothelial cells were randomly selected

per animal. All clearly defined fenestrae that were present along an endothelial cell membrane and were adjacent to the glomerular basement membrane were counted per image and designated as open or as containing electron dense material as a clearly visible black line, indicative of a diaphragm. The ratio of fenestra with or without apparent diaphragms per image was presented as a percentage for each image, and these values were used to determine the average percent of fenestra with diaphragms per genotype. In addition, the fenestral diameters were measured using TEM images, in which the plane of section across the fenestra was tangential (see Supplemental Figure 2). The diameter measurements recorded the shortest distance across individual fenestrae.

Immunofluorescence

Kidney tissue was excised from six animals (three pairs of gender matched littermates; 4 females and 2 males) that were 6 weeks old and fixed in 4% paraformaldehyde overnight. The tissue samples were then dehydrated using 15% sucrose overnight, followed by a second dehydration with 30% sucrose overnight. Tissue was then frozen in Neg50 and sectioned using a cryostat (8-micron sections). For immunofluorescence, slides were first blocked in 1% normal donkey serum in 0.5% Triton-X100 and 0.1% saponin in PBS (TSP) for 1 h at 37 °C. Next, the slides were incubated in primary antibody in blocking solution for 1 h at 37 °C, then washed with TSP and incubated in secondary antibody in blocking solution for 1 h at 37 °C. Finally, the slides were washed in TSP, stained with DAPI and mounted using Prolong Diamond.

Immunofluorescent images were captured with a Nikon Ni-E microscope with an Andor Zyla camera and analyzed using the Nikon NIS Elements Software. All images were collected at 60× as a z-stack. The image stack was then flattened using the focused image function found in the Elements software. Analysis of immunofluorescence images was done in a blinded manner. Under these conditions, we did not identify any evident changes in the distribution and appearance of the labeled cells or their spatial relationship to one another.

Histopathology

Kidney were harvested and fixed by immersion in 10% neutral buffered formalin, routinely processed in alcohol and xylene, embedded in paraffin, sectioned at 5 µm thickness and stained with hematoxylin and eosin (H&E). Slides were examined by a board-certified veterinary pathologist (SM).

Immunohistochemistry

After overnight fixation in 4% paraformaldehyde fixative, the kidneys of newborn mice were dehydrated and embedded in paraffin for CD31 staining. Slides with 5-micron sections were stained at the Memorial Sloan-Kettering Cancer Center Molecular Cytology Core Facility with Ventana staining processors (Ventana, Roche), using standard protocols with CD31 antibody (1 µg/ml, from Dianova, cat. # DIA-310). Stained slides were analyzed in a blinded manner. Several representative stages of kidney development (i.e., S-shaped bodies, maturing glomeruli and mature glomeruli) were identified and imaged per mouse. Those images were then again compared in a blinded manner. A total of six newborn mice were analyzed (3 pairs of littermates; each pair with one control and one mutant animal). The PLVAP staining was performed on frozen sections prepared from six mutant and littermate control mice (4 females and 2 males) that were 6 weeks old, and the bound secondary alkaline-phosphatase (AP)-labeled antibody was visualized by incubation with the AP substrates BCIP (5-bromo-4-chloro-3-indolyl phosphate) and NBT (nitro blue tetrazolium). NBT-BCIP (Roche) staining in NTMT (100 mM NaCl, 100 mM Tris-HCl pH9.5, 50 mM MgCl2, 1% Tween20, 20 µM Levamisole, in H_2O) occurred for 2 h at room temperature.

Lectin perfusion and light sheet microscopy

Newborn (postnatal day zero, P0) pups were anesthetized with a ketamine/xylazine cocktail (3 mutant mice and 3 littermate controls). Once fully anesthetized, the animals received an intracardiac injection of 100 µl of a solution that contained fluorescently tagged tomato lectin (Vector Laboratories DL-1178). A master solution was made of 880 µl of phosphate-buffered saline, 100 µl of fluorescently tagged lectin and 20 µl of heparin. The animal was left on a heating pad for 5 min to let the lectin circulate and then euthanized to harvest the kidneys.

The isolated kidneys were then cleared using the iDisco method of clearing, which uses graded series of methanol (20, 40, 60, 80, 100 and 100% all for 1 h), then dichloromethane (66% in 33% methanol for 1 h, followed by 100% for 20 min), and ending with dibenzyl ether (until the sample was clear) [44]. The cleared kidneys were imaged using a LaVision Ultramicroscope. The collected images were then analyzed using Imaris. Glomeruli in the samples shown in Fig. 5 were digitally removed to highlight the vascular branching pattern.

Glomeruli enrichment and qPCR

Adult kidneys were isolated from the euthanized 6-week-old animals (4 males and 2 females, gender matched littermates),

minced into small pieces and placed in a solution of PBS and 1 mg/ml collagenase A. The mixture was placed in a 37 °C water bath for 45 min and lightly vortexed every 5 min. Then, the resulting suspension was passed through a set of three wire mesh sieves with a decreasing size cutoff (first 250 µm, then 106 µm and then 53 µm, Endecotts Ltd, London, UK). Glomeruli that were collected on the surface of the 53-µm-mesh sieves were harvested, resuspended and disrupted by passing through a 1-ml syringe with a 22-G needle, and then RNA was isolated using RNeasy kit. qPCR genes for analysis were chosen based on known roles in endothelial Notch signaling, or in regulating vascular caliber or in production of fenestral diaphragms (see supplemental Table I for qPCR primers).

Measurement of proteinuria

Urine was collected for proteinuria measurements from all mice at 7–8 weeks of age (5 female control, 6 female mutant, 8 male control and 5 male mutant samples; from a total of 10 separate litters). Urinary creatinine concentration was measured using the Jaffé reaction. Proteinuria was assessed by SDS-PAGE of creatinine-adapted, desalted mouse urine as described previously [45]. Urine albumin content was quantified using a commercially available ELISA system (Bethyl), according to the manufacturer's instructions, using an ELISA plate reader (BioTek; EL 808), as described [45]. The urinary albumin concentration was calculated according to the formula for absorption $= (A\ 2\ D)/1 + (x/C)\ B + D)$, where A and D are values from the standard curve. Regression values for the standard curve with r values > 0.9950 indicated accurate measurements. Urinary albumin values were standardized against urine creatinine values of the same animals and plotted.

Serum analyses

Serum electrolyte (sodium, potassium, chloride and calcium), renal function parameters (creatinine and blood urea nitrogen (BUN)) and albumin concentrations from the same animals used for urinalysis (see above) were assessed by automated measurement at the department of Clinical Chemistry of the University Hospital Hamburg-Eppendorf.

Statistical analysis

Statistical analysis of images and qPCR was performed using GraphPad Prism software. When applicable, t tests were used to test for statistical significance. Statistical analysis of the urine samples was performed using the two-tailed nonparametric Mann–Whitney U test for comparison of *A10ΔEC* versus control littermates to enable robust conclusions on effects significance in case of departures from normality associated with small sample sizes. Replicates used were biological replicates, which were measured using different samples derived from distinct mice. All animals were littermates and were blindly assigned to the experimental groups. No inclusion or exclusion criteria were defined for animals, and no animals were excluded from the analysis. Group measures are given as mean ± SEM. A p value of < 0.05 was considered statistically significant.

Acknowledgements G. Farber is currently supported by a predoctoral Fellowship from the American Heart Association and was previously supported by Molecular and Cellular Biology T32 training Grant from the National Institutes of Health, 5T32GM008539. These studies were supported in part by the National Institutes of Health R01 Grant GM64750 to CPB. We would like to thank Dr. Alison North and Rockefeller University's Bio-Imaging Resource Center for the training and usage of the light sheet microscopy and image analysis, Dr. Kunihiro Uryu and Rockefeller University's Electron Microscopy Resource Center for training on and usage of scanning electron microscopy. A special thanks to Lee Cohen Gould and Juan Jimenez at the Weill Cornell Medicine Imaging Core Facility for the preparation of the transmission electron microscopy samples and training, and Dr. Katia Manova, Ning Fan and Afsar Barlas from the Molecular Cytology Core Facility at Memorial Sloan-Kettering Cancer Center (supported by the Cancer Center Support Grant P30CA008748). S. Monette and the Laboratory of Comparative Pathology are also supported in part by Cancer Center Support Grant P30CA008748.

Author's Contribution GF and CB conceived of this study, RH, SL, SM, JM and CMS performed experiments and interpreted the results, GF drafted the manuscript, all authors contributed to editing, and GF and RPS prepared the figures.

Compliance with Ethical Standards

Conflict of interest The authors declare that they have no conflict of interest.

References

1. Scott RP, Quaggin SE (2015) Review series: the cell biology of renal filtration. J Cell Biol 209(2):199–210. https://doi.org/10.1083/jcb.201410017
2. Eremina V, Baelde HJ, Quaggin SE (2007) Role of the VEGF-A signaling pathway in the glomerulus: evidence for crosstalk between components of the glomerular filtration barrier. Nephron Physiol 106(2):p32–p37. https://doi.org/10.1159/000101798
3. Vaughan MR, Quaggin SE (2008) How do mesangial and endothelial cells form the glomerular tuft? J Am Soc Nephrol 19(1):24–33. https://doi.org/10.1681/ASN.2007040471
4. Ichimura K, Stan RV, Kurihara H, Sakai T (2008) Glomerular endothelial cells form diaphragms during development and pathologic conditions. J Am Soc Nephrol 19(8):1463–1471. https://doi.org/10.1681/ASN.2007101138
5. Satchell SC, Braet F (2009) Glomerular endothelial cell fenestrations: an integral component of the glomerular filtration barrier. Am J Physiol Renal Physiol 296(5):F947–F956. https://doi.org/10.1152/ajprenal.90601.2008
6. Stan RV (2007) Endothelial stomatal and fenestral diaphragms in normal vessels and angiogenesis. J Cell Mol Med 11(4):621–643. https://doi.org/10.1111/j.1582-4934.2007.00075.x

7. Wang Y, Rattner A, Zhou Y, Williams J, Smallwood PM, Nathans J (2012) Norrin/Frizzled4 signaling in retinal vascular development and blood brain barrier plasticity. Cell 151(6):1332–1344. https://doi.org/10.1016/j.cell.2012.10.042
8. Covassin L, Amigo JD, Suzuki K, Teplyuk V, Straubhaar J, Lawson ND (2006) Global analysis of hematopoietic and vascular endothelial gene expression by tissue specific microarray profiling in zebrafish. Dev Biol 299(2):551–562. https://doi.org/10.1016/j.ydbio.2006.08.020
9. Chang AC, Fu Y, Garside VC, Niessen K, Chang L, Fuller M, Setiadi A, Smrz J, Kyle A, Minchinton A, Marra M, Hoodless PA, Karsan A (2011) Notch initiates the endothelial-to-mesenchymal transition in the atrioventricular canal through autocrine activation of soluble guanylyl cyclase. Dev Cell 21(2):288–300. https://doi.org/10.1016/j.devcel.2011.06.022
10. Mintet E, Lavigne J, Paget V, Tarlet G, Buard V, Guipaud O, Sabourin JC, Iruela-Arispe ML, Milliat F, Francois A (2017) Endothelial Hey2 deletion reduces endothelial-to-mesenchymal transition and mitigates radiation proctitis in mice. Sci Rep 7(1):4933. https://doi.org/10.1038/s41598-017-05389-8
11. Quaggin SE, Kreidberg JA (2008) Development of the renal glomerulus: good neighbors and good fences. Development 135(4):609–620. https://doi.org/10.1242/dev.001081
12. Boyle SC, Liu Z, Kopan R (2014) Notch signaling is required for the formation of mesangial cells from a stromal mesenchyme precursor during kidney development. Development 141(2):346–354. https://doi.org/10.1242/dev.100271
13. Cheng HT, Kopan R (2005) The role of Notch signaling in specification of podocyte and proximal tubules within the developing mouse kidney. Kidney Int 68(5):1951–1952. https://doi.org/10.1111/j.1523-1755.2005.00627.x
14. Glomski K, Monette S, Manova K, De Strooper B, Saftig P, Blobel CP (2011) Deletion of Adam10 in endothelial cells leads to defects in organ-specific vascular structures. Blood 118(4):1163–1174. https://doi.org/10.1182/blood-2011-04-348557
15. Bozkulak EC, Weinmaster G (2009) Selective use of ADAM10 and ADAM17 in activation of Notch1 signaling. Mol Cell Biol 29(21):5679–5695
16. van Tetering G, van Diest P, Verlaan I, van der Wall E, Kopan R, Vooijs M (2009) Metalloprotease ADAM10 is required for Notch1 site 2 cleavage. J Biol Chem 284(45):31018–31027
17. Rooke J, Pan D, Xu T, Rubin GM (1996) KUZ, a conserved metalloprotease-disintegrin protein with two roles in Drosophila neurogenesis. Science 273(5279):1227–1230
18. Hartmann D, de Strooper B, Serneels L, Craessaerts K, Herreman A, Annaert W, Umans L, Lubke T, Lena Illert A, von Figura K, Saftig P (2002) The disintegrin/metalloprotease ADAM 10 is essential for Notch signalling but not for alpha-secretase activity in fibroblasts. Hum Mol Genet 11(21):2615–2624
19. Alabi RO, Glomski K, Haxaire C, Weskamp G, Monette S, Blobel CP (2016) ADAM10-dependent signaling through Notch1 and Notch4 controls development of organ-specific vascular beds. Circ Res 119(4):519–531. https://doi.org/10.1161/CIRCRESAHA.115.307738
20. Gridley T (2007) Notch signaling in vascular development and physiology. Development 134(15):2709–2718
21. Hellstrom M, Phng LK, Hofmann JJ, Wallgard E, Coultas L, Lindblom P, Alva J, Nilsson AK, Karlsson L, Gaiano N, Yoon K, Rossant J, Iruela-Arispe ML, Kalen M, Gerhardt H, Betsholtz C (2007) Dll4 signalling through Notch1 regulates formation of tip cells during angiogenesis. Nature 445(7129):776–780
22. Hofmann JJ, Iruela-Arispe ML (2007) Notch signaling in blood vessels: Who is talking to whom about what? Circ Res 100(11):1556–1568. https://doi.org/10.1161/01.RES.0000266408.42939.e4
23. Roca C, Adams RH (2007) Regulation of vascular morphogenesis by Notch signaling. Genes Dev 21(20):2511–2524
24. Kusumbe AP, Ramasamy SK, Adams RH (2014) Coupling of angiogenesis and osteogenesis by a specific vessel subtype in bone. Nature 507(7492):323–328. https://doi.org/10.1038/nature13145
25. Ramasamy SK, Kusumbe AP, Wang L, Adams RH (2014) Endothelial Notch activity promotes angiogenesis and osteogenesis in bone. Nature 507(7492):376–380. https://doi.org/10.1038/nature13146
26. Cuervo H, Nielsen CM, Simonetto DA, Ferrell L, Shah VH, Wang RA (2016) Endothelial notch signaling is essential to prevent hepatic vascular malformations in mice. Hepatology. https://doi.org/10.1002/hep.28713
27. Blanco R, Gerhardt H (2013) VEGF and Notch in tip and stalk cell selection. Cold Spring Harb Perspect Med 3(1):a006569. https://doi.org/10.1101/cshperspect.a006569
28. Takemoto M, Asker N, Gerhardt H, Lundkvist A, Johansson BR, Saito Y, Betsholtz C (2002) A new method for large scale isolation of kidney glomeruli from mice. Am J Pathol 161(3):799–805. https://doi.org/10.1016/S0002-9440(10)64239-3
29. Stan RV, Tkachenko E, Niesman IR (2004) PV1 is a key structural component for the formation of the stomatal and fenestral diaphragms. Mol Biol Cell 15(8):3615–3630. https://doi.org/10.1091/mbc.E03-08-0593
30. Ioannidou S, Deinhardt K, Miotla J, Bradley J, Cheung E, Samuelsson S, Ng YS, Shima DT (2006) An in vitro assay reveals a role for the diaphragm protein PV-1 in endothelial fenestra morphogenesis. Proc Natl Acad Sci USA 103(45):16770–16775. https://doi.org/10.1073/pnas.0603501103
31. Kidoya H, Ueno M, Yamada Y, Mochizuki N, Nakata M, Yano T, Fujii R, Takakura N (2008) Spatial and temporal role of the apelin/APJ system in the caliber size regulation of blood vessels during angiogenesis. EMBO J 27(3):522–534. https://doi.org/10.1038/sj.emboj.7601982
32. Takakura N, Kidoya H (2009) Maturation of blood vessels by haematopoietic stem cells and progenitor cells: involvement of apelin/APJ and angiopoietin/Tie2 interactions in vessel caliber size regulation. Thromb Haemost 101(6):999–1005
33. Kidoya H, Takakura N (2012) Biology of the apelin-APJ axis in vascular formation. J Biochem 152(2):125–131. https://doi.org/10.1093/jb/mvs071
34. Shawber CJ, Funahashi Y, Francisco E, Vorontchikhina M, Kitamura Y, Stowell SA, Borisenko V, Feirt N, Podgrabinska S, Shiraishi K, Chawengsaksophak K, Rossant J, Accili D, Skobe M, Kitajewski J (2007) Notch alters VEGF responsiveness in human and murine endothelial cells by direct regulation of VEGFR-3 expression. J Clin Invest 117(11):3369–3382. https://doi.org/10.1172/JCI24311
35. Takabatake Y, Sugiyama T, Kohara H, Matsusaka T, Kurihara H, Koni PA, Nagasawa Y, Hamano T, Matsui I, Kawada N, Imai E, Nagasawa T, Rakugi H, Isaka Y (2009) The CXCL12 (SDF-1)/CXCR4 axis is essential for the development of renal vasculature. J Am Soc Nephrol 20(8):1714–1723. https://doi.org/10.1681/ASN.2008060640
36. Makanya AN, Stauffer D, Ribatti D, Burri PH, Djonov V (2005) Microvascular growth, development, and remodeling in the embryonic avian kidney: the interplay between sprouting and intussusceptive angiogenic mechanisms. Microsc Res Tech 66(6):275–288. https://doi.org/10.1002/jemt.20169
37. Notoya M, Shinosaki T, Kobayashi T, Sakai T, Kurihara H (2003) Intussusceptive capillary growth is required for glomerular repair in rat Thy-1.1 nephritis. Kidney Int 63(4):1365–1373. https://doi.org/10.1046/j.1523-1755.2003.00876.x
38. Foster RR, Slater SC, Seckley J, Kerjaschki D, Bates DO, Mathieson PW, Satchell SC (2008) Vascular endothelial growth

factor-C, a potential paracrine regulator of glomerular permeability, increases glomerular endothelial cell monolayer integrity and intracellular calcium. Am J Pathol 173(4):938–948. https://doi.org/10.2353/ajpath.2008.070416

39. Benedito R, Rocha SF, Woeste M, Zamykal M, Radtke F, Casanovas O, Duarte A, Pytowski B, Adams RH (2012) Notch-dependent VEGFR3 upregulation allows angiogenesis without VEGF-VEGFR2 signalling. Nature 484(7392):110–114. https://doi.org/10.1038/nature10908
40. Coon BG, Baeyens N, Han J, Budatha M, Ross TD, Fang JS, Yun S, Thomas JL, Schwartz MA (2015) Intramembrane binding of VE-cadherin to VEGFR2 and VEGFR3 assembles the endothelial mechanosensory complex. J Cell Biol 208(7):975–986. https://doi.org/10.1083/jcb.201408103
41. Djonov VG, Kurz H, Burri PH (2002) Optimality in the developing vascular system: branching remodeling by means of intussusception as an efficient adaptation mechanism. Dev Dyn 224(4):391–402. https://doi.org/10.1002/dvdy.10119
42. Wasserman SM, Mehraban F, Komuves LG, Yang RB, Tomlinson JE, Zhang Y, Spriggs F, Topper JN (2002) Gene expression profile of human endothelial cells exposed to sustained fluid shear stress. Physiol Genomics 12(1):13–23. https://doi.org/10.1152/physiolgenomics.00102.2002
43. Kim YH, Hu H, Guevara-Gallardo S, Lam MT, Fong SY, Wang RA (2008) Artery and vein size is balanced by Notch and ephrin B2/EphB4 during angiogenesis. Development 135(22):3755–3764. https://doi.org/10.1242/dev.022475
44. Renier N, Adams EL, Kirst C, Wu Z, Azevedo R, Kohl J, Autry AE, Kadiri L, Umadevi Venkataraju K, Zhou Y, Wang VX, Tang CY, Olsen O, Dulac C, Osten P, Tessier-Lavigne M (2016) Mapping of brain activity by automated volume analysis of immediate early genes. Cell 165(7):1789–1802. https://doi.org/10.1016/j.cell.2016.05.007
45. Meyer TN, Schwesinger C, Wahlefeld J, Dehde S, Kerjaschki D, Becker JU, Stahl RA, Thaiss F (2007) A new mouse model of immune-mediated podocyte injury. Kidney Int 72(7):841–852. https://doi.org/10.1038/sj.ki.5002450